Journal of Materials Science: Materials in Electronics (2018) 29:3744–3750
https://doi.org/10.1007/s10854-017-8308-1

Electric and dielectric properties of ytterbium substituted spinel ferrites

Kalsoom Bibi[1] · Irshad Ali[2] · Muhammad Tahir Farid[2] · Asif Mahmood[3] · Shahid M. Ramay[4] · Khuram Ali[5]

Received: 21 September 2017 / Accepted: 20 November 2017 / Published online: 30 November 2017

Abstract
Ytterbium (Yb) substituted magnesium ferrite materials ($MgYb_xFe_{2-x}O_4$ with x = 0.00, 0.025, 0.050, 0.075, 0.10) have been prepared by the Sol–gel method. XRD analysis revealed that the prepared samples are cubic spinel with single phase till the content 'x' equals 0.05. At higher content $x \geq 0.075$, Yb substituted samples possessed $YbFeO_3$ phase along with the cubic spinel phase. A significant decrease of ~34.7 nm in crystallite size is noted in response to the increase in Yb substitution level. The room temperature dc resistivity increases gradually from 3.47×10^7 to 2.63×10^8 Ω-cm as the substitution of Yb is increased. Temperature dependent DC electrical resistivity of all the samples exhibits semiconducting behavior. Yb substituted materials can be suitable to limit the eddy current losses for microwave applications. VSM indicated the existence of an appreciable fraction of ferrimagnetic properties at room temperature. The saturation magnetization of the samples decreases from 60 to 33 emu/g. Saturation magnetization and remanence decreased while coercivity increased with Yb substitution.

1 Introduction

Ferrites are very applicable in technological fields with regards to fine size distribution and its identical particle size. The important factors which affect the structural as well as electrical properties of spinel ferrites are the sintering temperature, site occupancy of parents materials, substitution of host materials and method through which these spinel ferrites are prepared [1]. Ferrites are more applicable as a good dielectric material and very useful for microwave devices also [1]. Spinel ferrites of the general formula, MFe_2O_4 (Mg^{2+}, Co^{2+}, Mn^{2+}, etc.) having their effective use in different fields like magnetic refrigeration and storage devices due to their low cost and adopting the easy method for their preparation [2, 3].

In Spinel ferrites, Mg-based spinel ferrites have their special attention due to low dielectric and magnetic loss. They also possessed high value of resistivity [4, 5]. Besides, due to its interesting properties as a result of substitutions at Mg^{2+} and Fe^{3+} sites, many researchers have been attracted to explain this ferrite material, especially its magnetic properties based on Fe^{3+} distribution in the tetrahedral and octahedral sites [6]. There are different properties of spinel ferrites like magnetic and electrical properties through which one can able to measure the position of ions on tetrahedral or octahedral site and conduction mechanism. Few authors had already discussed the magnetic, electric, dielectric and structural properties of Mg-based spinel ferrites with substitution like Zn^{2+} [7], Cd^{2+} [8], Ti^{2+} [9] and Al^{3+} [10].

The substitution of rare earth in $MgFe_2O_4$ is considered the best method to modify the properties of ferrites, as was done recently with Praseodymium [11]. But a study of physical, electrical and magnetic properties of Ytterbium substituted magnesium ferrite using sol–gel is not yet reported. So the present work an investigation on the effect of Yb substitution in structural, electrical and magnetic properties of magnesium ferrite is attempted.

In this work, we prepared $MgYb_xFe_{2-x}O_4$ compounds containing different levels of Yb (x = 0.00, 0.025, 0.05, 0.075,

✉ Irshad Ali
irshadalibzu@gmail.com

1 Department of Physics, Allama Iqbal Open University, Islamabad, Pakistan

2 Department of Physics, Bahauddin Zakariya University, Multan 60800, Pakistan

3 Chemical Engineering Department, College of Engineering, King Saud University, Riyadh, Saudi Arabia

4 Physics and Astronomy Department, College of Science, King Saud University, P.O. Box 2455, Riyadh 11451, Saudi Arabia

5 Nano-optoelectronics Research Laboratory, Department of Physics, University of Agriculture, Faisalabad, Faisalabad 38040, Pakistan

0.10), and effect on structural, morphological, electrical and magnetic properties by substitution of Yb^{3+} ions into host materials Fe^{3+}. The aim of Yb^{3+} substitution is to reduce eddy current loss, enhance DC-electrical resistivity and magnetic properties for microwave and recording media application.

2 Experimental

Mg-based spinel ferrites were prepared by wet method (sol–gel auto combustion technique). For this purpose, initially 99.99% pure following nitrates of Yb $(NO_3)_3$, Fe $(NO_3)_3$ and Mg $(NO_3)_2$ were put in de-ionized water of 100 ml in Pyrex beaker to dissolve their measured quantities. To get the homogeneous and nano-structured spinel ferrites, citric acid worked as chelating agency. This whole solution was put on magnetic stirrer by applying the constant temperature of 80 °C to get the homogeneous mixture. To maintain the pH scale of homogeneous mixture at 7, drop by drop ammonia solution was added. After 3–4 h the whole mixture adopted the shape of viscous gel. The self combustion process of that viscous gel was started at 370 °C when it was placed in furnace. Within few minutes, this whole viscous gel was converted into precursor powder. With the help of mortar-piston, this whole precursor powder was grounded and then it is placed in furnace for 5 h at 700 °C for pre-sintering process. All the samples were annealed. To prepare the mixture for pellets, Polyvinyl binder was added into the mixture. With the help of Hydraulic press, pellets were formed by applying the load of 30 kN. Then all the samples were placed in furnace for one hour at 250 °C to remove the binder. The prepared pellets of all the samples were finally sintered at 950 °C for 7 h.

The lattice parameter "a" of spinel ferrites was extracted from the X-ray diffraction analysis by using the hkl values with the help of equation [11]

$$a = d_{hkl}\sqrt{h^2 + k^2 + l^2} \tag{1}$$

The X-ray density of all the prepared spinel ferrites was calculated from lattice constant 'a' and molar mass 'M' of the samples with the help of the following equation: [11]

$$\mathrm{D_X} = \frac{8M}{N_A a^3} \tag{2}$$

where 'N_A' is the constant called Avogadro's number.

The bulk density of all the samples was measured by using this relation [11]

$$D_m = \frac{8M}{\pi l r^2} \tag{3}$$

The porosity of all the samples was calculated by using the values of X-ray density and bulk density by using this equation [11].

$$\mathrm{P} = 1 - \left(\frac{D_m}{D_x}\right) \tag{4}$$

By using the effective area of the electrode in contact with the sample 'A', the thickness of each sample 'ℓ' and resistance of the materials, the values of resistivity can be calculated by using this formula [11].

$$\rho = \frac{RA}{\ell} \tag{5}$$

The activation energy was calculated from the slope of the graphs between log ρ versus $1000/T$ by using equation [11].

$$\rho = \rho_o \exp\left(\frac{\Delta E}{K_B T}\right) \tag{6}$$

where ρ is resistivity, K_B is for Boltzmann's constant and "ΔE" *represents the* activation energy of the hopping mechanism of electrons from one metal ion to the adjacent neighbor ion.

3 Results and discussions

3.1 Structural properties

Structural properties of spinel ferrites were analyzed from X-ray diffraction analysis and scanning electron microscopy. The X-ray diffraction analysis of spinel ferrites with formula $MgYb_xFe_{2-x}O_4$ (x = 0.00, 0.025, 0.05, 0.075, 0.10) was performed in the range of 2θ from 10° to 69.9° with the help of Bruker axis D8 diffractometer by using Cu-kα (λ = 1.5406 Å) radiation.

Figure 1 shows that diffraction peaks of all the samples becoming broader and narrow with the substitution of Ytterbium. These corresponding planes of these diffraction peaks having Miller indices (220), (311), (222), (400), (422), (511/333), (440). These values of peaks proved that the prepared ferrites possessed the cubic spinel phase. At high concentration (x ≥ 0.075), two more peaks are observed at 2θ = 32.4° and 45.4° having hkl values (211) and (311) respectively. These peaks are identified as $YbFeO_3$ (iron ytterbium oxide) matched with ICDDPDF # 39-1489. This kind of secondary phase with the substitution of rare earth ions was also observed by [12, 13]. The intensity of these two peaks is increasing with the substitution of Ytterbium ions.

The lattice constant was calculated by using Eq. 1. The graph between the lattice constant as a function of Yb concentration is shown in Fig. 2. The linear increase in lattice constant has been observed with the substitution of Yb contents. It can be explained by this fact that the Yb has a larger

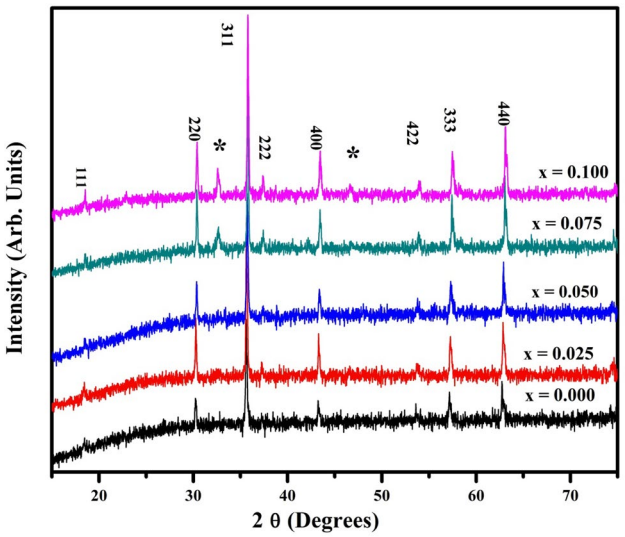

Fig. 1 X-Ray diffraction patterns of $MgYb_xFe_{2-x}O_4$ spinel ferrites

ionic radius as compared to iron ions. When Yb of relative larger radius replaces the iron ions, the value of lattice constant is increased. At high concentration ($x \geq 0.075$), the value of lattice constant is also increasing because the spinel lattice is not compressed with the substitution of Yb contents forming the secondary phase. This second phase is highly resistive in nature. Such type of results is also observed by different researchers [14, 15].

By using the Eqs. 2 and 3, X-ray density and bulk density of all the samples were measured. There was a linear incease in both densities as shown in Fig. 3. It can be observed that, as the substitution of 'Yb' is increasing, both densities also increased and become maximum at $x = 0.10$. This increase in both densities is due to the difference in molar solutions of rare earth and iron ions. The molar volume of rare earth is much larger as compared to iron ions.

The % porosity of each sample was extracted from the data of X-ray density and bulk density by using Eq. 4. As comparatively, bulk density of each sample is smaller than corresponding X-ray density. The calculated values of % porosity are presented in Table 1.

3.2 Scanning electron microscopy (SEM)

The SEM images of all the prepared spinel ferrites $MgYb_xFe_{2-x}O_4$ ($x = 0.00, 0.025, 0.05, 0.075, 0.10$) have been presented in Fig. 4. The grains of all the samples are uniformly distributed and possessed spherical shape. The grain size was calculated by slope intercept method.

The values of grain size decrease from 53.2 to 34.7 nm as the substitution of Yb concentration is enhanced from 0.00 to 0.10. It can be observed from Table 1, as the substitution of Y_b is increased, the grain size decreases continuously. Such types of results are also reported by [16, 17].

3.3 Electrical properties

The property of prepared material through which it opposes the motion of free electrons is known as resistivity. The electrical resistivity of the material is changed with the substitution of rare earth ions into Mg-bases material as well as by changing the temperature [18].

Electrical resistivity of $MgYb_xFe_{2-x}O_4$ ($x = 0.00, 0.025, 0.05, 0.075, 0.10$) spinel ferrites was experimentally measured at room temperature with the help of Eq. 5. The values of dc resistivity are enhanced from 3.47×10^7 to 2.63×10^8 Ω-cm as the substitution of Yb is increased. The rare earth material 'Yb' is more resistive as compared to iron

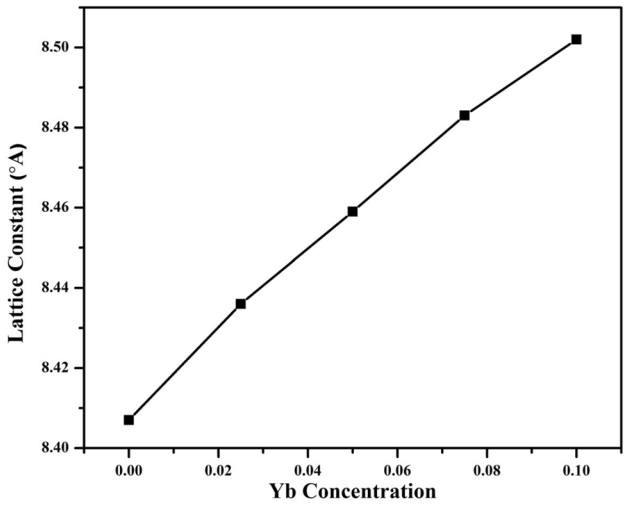

Fig. 2 Lattice constant versus Yb-concentration for $MgYb_xFe_{2-x}O_4$ spinel ferrites

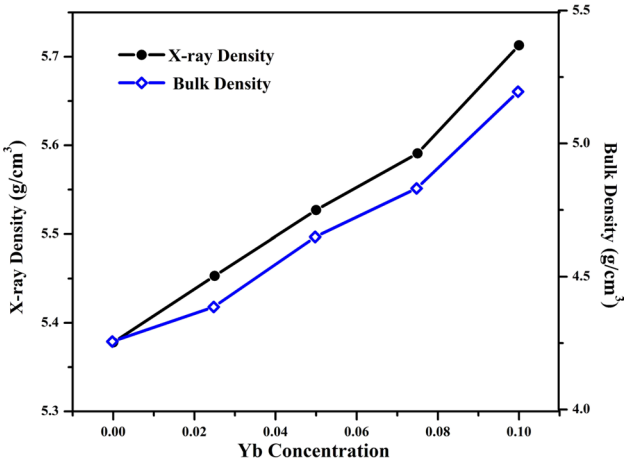

Fig. 3 X-ray density and bulk density versus Yb concentration

Table 1 Compositional variation of crystallite size, porosity, activation energy, dielectric constant, dielectric loss and remanence of $MgYb_xFe_{2-x}O_4$ spinel ferrites

Composition	x = 0.00	x = 0.025	x = 0.05	x = 0.075	x = 0.10
Crystallite size (nm)	53.2	51.4	48.3	42.8	34.7
Porosity (%P)	20.863	19.569	15.886	13.594	9.068
Activation energy E_a (eV)	0.16723	0.1709	0.18041	0.18558	0.18838
Dielectric constant at 1 MHz	16.254	12.642	9.3623	7.644	5.6448
Dielectric loss at 1 MHz	1.47429	1.29714	1.13657	0.99086	0.89143
Remanence (emu/g)	20.1	18.3	15.4	13.2	12.7

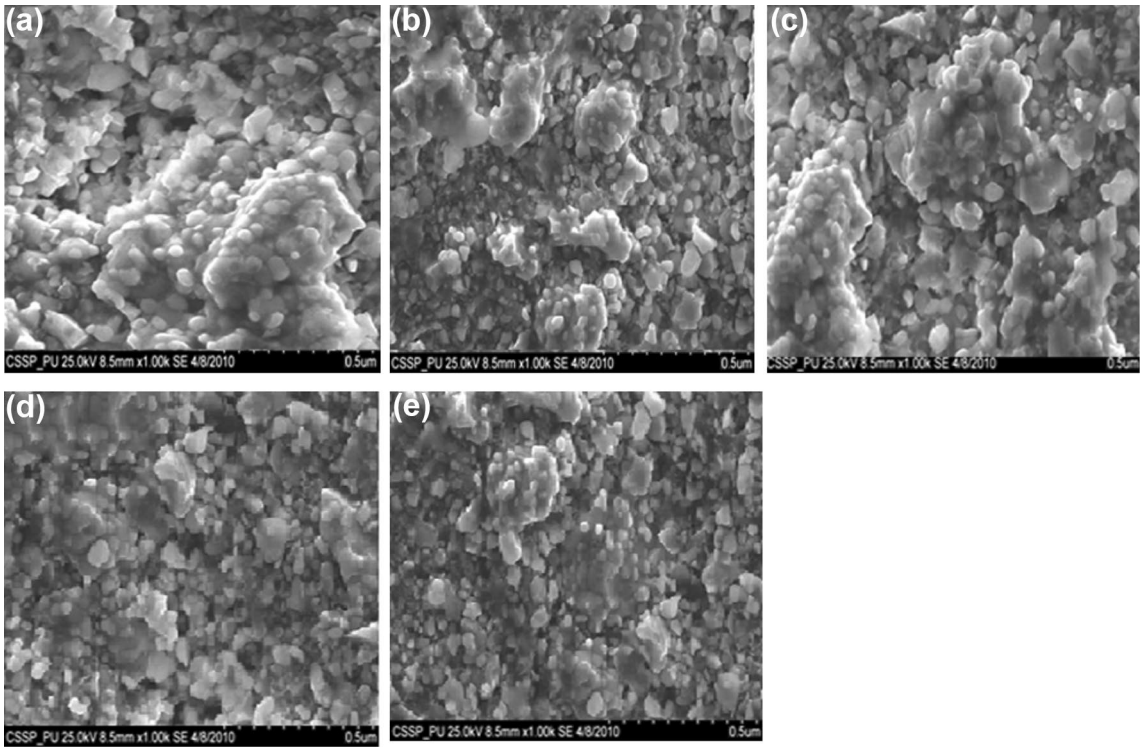

Fig. 4 SEM image $MgYb_xFe_{2-x}O_4$ spinel ferrites

ions. The graph between room temperature resistivity and 'Yb' concentration is shown in Fig. 5. It can be observed that the resistivity of last two samples ($x \geq 0.075$) is very high due to secondary phase, which formed the insulating layer. Few researchers [19–21] also reported such type of results. In spinel ferrites, there are tetrahedral (A-site) and octahedral (B-site) sites. The rare earth element possessed the B-site. The substitution of Yb ions replaces the iron ions from B-site. It impedes the hopping of charge carriers between tetrahedral and octahedral sites. Hence the resistivity of the prepared samples is enhanced.

Temperature dependent dc resistivity of all the samples was calculated in the range of 300–693 K and presented in Fig. 6. The Arrhenius plot was presented between ln ρ and 1000/T. It can be observed from the Fig. 6 that dc resistivity of the prepared samples decreases with the increase in temperature. So the semiconducting nature of materials has been

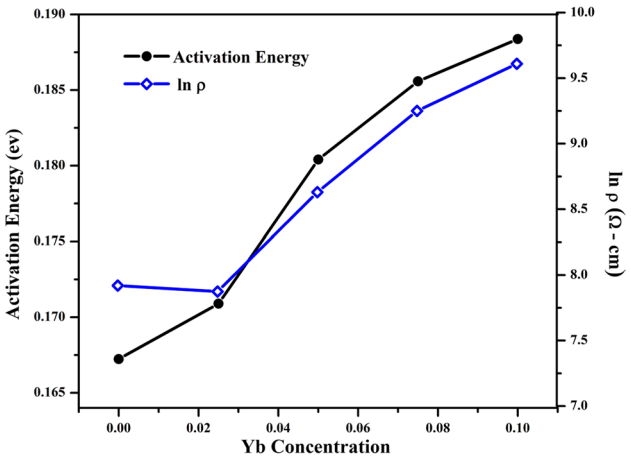

Fig. 5 Room temperature resistivity and activation energy versus Yb-concentration (x) for $MgYb_xFe_{2-x}O_4$ spinel ferrites

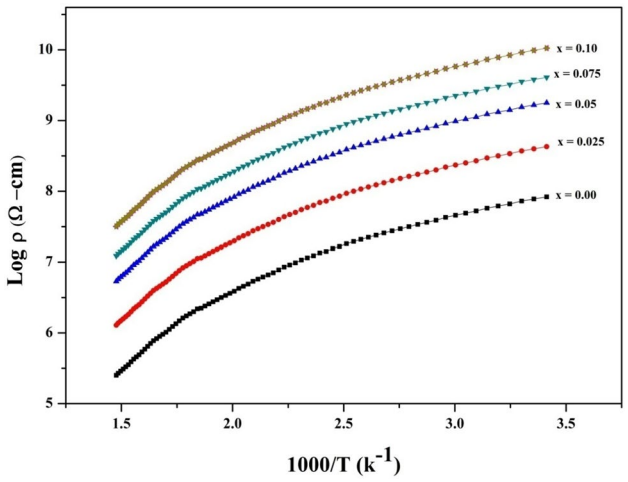

Fig. 6 The log dc resistivity as a function of temperature for $MgYb_xFe_{2-x}O_4$ spinel ferrites

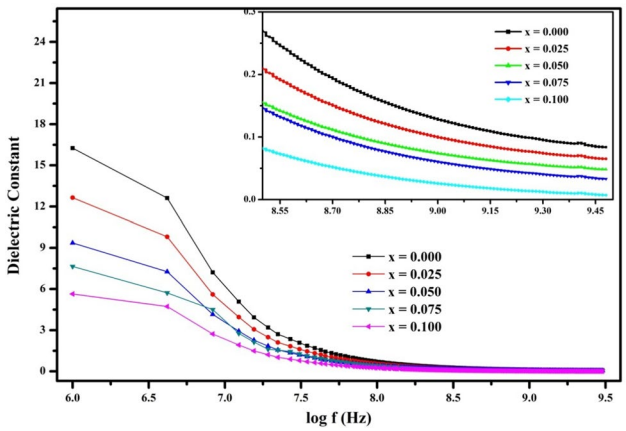

Fig. 7 Dielectric constant versus log frequency (Hz) for $MgYb_xFe_{2-x}O_4$ spinel ferrites

proved. As the temperature of spinel ferrites is enhanced, the hopping of electrons between Fe^{2+} and Fe^{3+} ions and jumping of holes Mg^{1+} and Mg^{2+} increase the conductivity of the materials [22, 23].

The activation energy of all the samples was calculated from Arrhenius equation which is labeled as 6. The values of activation energies lie in the range of 0.16–0.18 eV are presented in Table 1. It has been observed that activation energy has the same trend as that of room temperature resistivity. So the sample which possessed a low value of activation energy has a low value of resistivity and vice versa [24].

3.4 Dielectric properties

The dielectric constant and dielectric loss of all prepared spinel ferrites were determined in the frequency range of 1 MHz–3 GHz. It can be observed from Table 1 that as the concentration of Yb is increasing, the value of dielectric constant as well as well as the dielectric loss is decreased. From literature, it has been proved that the rare earth ions occupied the octahedral site.

The substitution of Yb ions decreases the concentration of Fe^{3+} ions from the octahedral site; hence electrical conductivity is reduced and both dielectric constant and dielectric loss have been decreased. The transfer of electrons between tetrahedral and octahedral site will be hindered and polarization of spinel ferrites is decreased. A similar trend has been observed by [25, 26]. The sample which contains a high value of dielectric constant possessed low value of conductivity. Hence the product of dielectric constant and square root of dc resistivity almost remains constant.

The frequency dependent graphs of dielectric constant are presented in Fig. 7. All the samples have an almost same trend. Initially, as the value of the applied field is low, the values of dielectric constants are larger. As the frequency is decreasing, the values of dielectric constants are rapidly decreased. While at higher frequencies, the graph of dielectric constant almost become constant. This observed behavior is quite general in spinel ferrites. According to Koop's theory, spinel ferrites are composed of highly conducting grains and resistive grain boundaries.

At a low value of frequency, charges are settled on the surface and space charge polarization is built up [27, 28]. The direction of motion of electrons has been reversed with the increase of reversal frequency of applied field. Due to this reason, chances of accumulation of charges at grain boundaries have been reduced, hence the polarization has been decreased. Therefore dielectric constant attained almost constant value at high frequencies.

The dielectric loss measured that how much amount of energy has been dissipated with the applied field [23]. The graph between imaginary part of permittivity and frequency (1 MHz–3 GHz) of all spinel ferrites have been plotted in Fig. 8. The dielectric loss has the same trend as the dielectric constant.

The sample which has a low value of dielectric loss possessed the high value of resistivity. So these prepared spinel ferrites are might be suitable for high-frequency applications.

3.5 Magnetic properties

The magnetic properties of $MgYb_xFe_{2-x}O_4$ (x = 0.00, 0.025, 0.05, 0.075, 0.10) spinel ferrites were measured experimentally by magnetometer. Here the magnetic field from − 2000 Oe to + 2000 Oe has been applied to prepared samples. M-H loops of all the samples were plotted in Fig. 9. It can be observed from the Fig. 9 that all the loops are narrow,

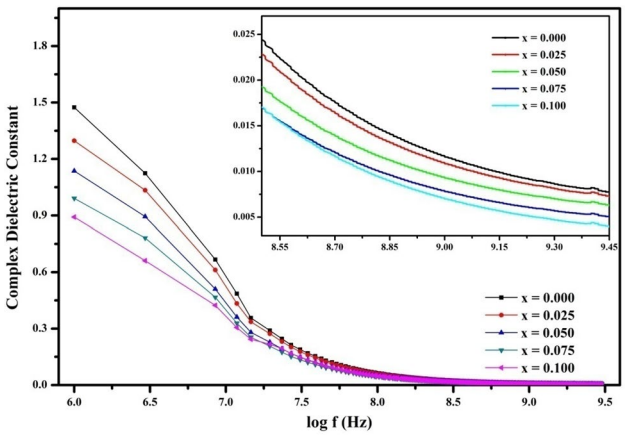

Fig. 8 Complex dielectric constant versus log frequency (Hz) for $MgYb_xFe_{2-x}O_4$ spinel ferrites

possessing soft nature of ferrites. From M-H loops, magnetic parameters like saturation magnetization, remanence and coercivity were measured.

The values of saturation magnetization and remanence lie in the range of 60–33 emu/g and 20–10 emu/g respectively. It has been observed that as the substitution of rare earth ions is increased the M_s as well as M_r decrease continuously. As the substitution of Yb ions is increased, it replaces the iron ions from the octahedral site. And net magnetization of the spinel ferrites has been decreased. Actually, the value of the magnetic moment of Y_b is lower as compared to Fe^{3+}. Similar results have been observed by [11].

Coercivity of the spinel ferrites lies between 159 Oe and 360 Oe. As the Yb concentration is increased, the values of coercivity are increased. According to Brown's relation [17], saturation magnetization and coercivity have an inverse relation as shown in Fig. 10. The sample which possessed a low value of saturation magnetization has a high value of coercivity. Different researchers have also proved such type of behavior.

4 Conclusions

Yttrium substituted copper-based spinel ferrites have been successfully synthesized and their magnetic, structural and electrical properties have been discussed in details. Structural properties revealed that all the prepared samples have cubic spinel structure while last two samples possessed few traces of secondary phase (orthorhombic) along spinel phase. There is linear increase in lattice constant with the substitution of rare-earth ions. Bulk density and X-ray density both increased with the increase of Yb concentration while porosity has been decreased. SEM images possessed inhomogeneous grain size. Room temperature dc resistivity of $MgYb_xFe_{2-x}O_4$ ferrites increases linearly. Temperature dependent dc electrical resistivity decreases as the temperature increases which is indicating semiconductor behavior of the samples. It was concluded that samples having low resistivity have low activation energy and vice versa. Dielectric constant and dielectric loss factor decrease with the increase in frequency. Magnetic properties showed that saturation magnetization and remanence increased with the increase of Yb concentration while coercivity has been decreased. All these parameters suggested that prepared spinel ferrites might be suitable for high-frequency applications.

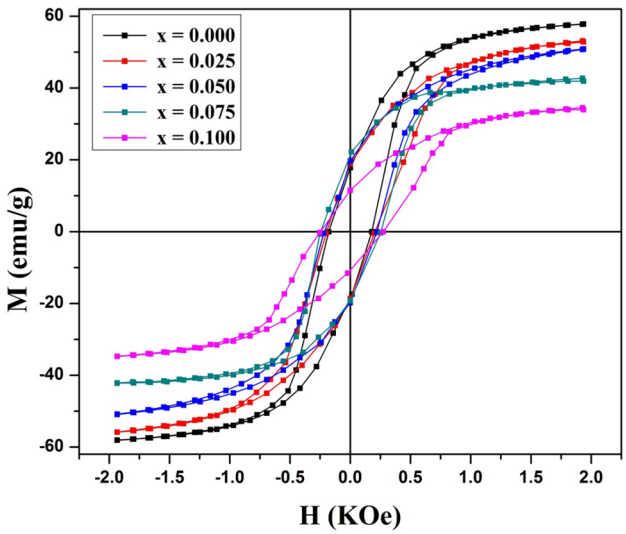

Fig. 9 M-H loops for $MgYb_xFe_{2-x}O_4$ spinel ferrites

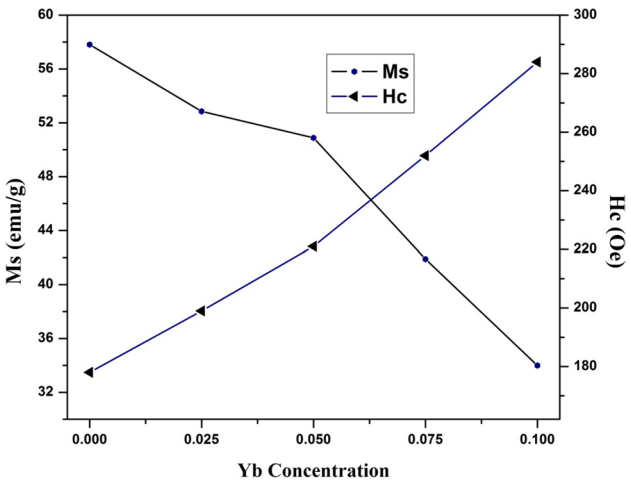

Fig. 10 Saturation magnetization and coercivity versus Yb- concentration for $MgYb_xFe_{2-x}O_4$ spinel ferrites

Acknowledgements The authors would like to extend sincere appreciation to the Deanship of Scientific Research at King Saud University for funding the work through the research group Project No. RGP-311.

References

1. M. Shahid, A. Ramay, N.S. Mahmood, A.S. Alzayed, S. Qaid, I. Ali, M.T. Farid, J. Mater. Sci. **28**, 18656–18665 (2017)
2. A.K. Giri, E.M. Kirkpatrick, P. Moongkhamklang, S.A. Majetich, Appl. Phys. Lett. **80**, 2341–2343 (2002)
3. M.F. Hansen, S. Morup, J. Magn. Magn. Mater. **184**, 262–274 (1998)
4. L.B. Kong, Z.W. Li, G.Q. Lin, Y.B. Gan, J. Am. Ceram. Soc. **90**, 2104–2112 (2007)
5. Y. Konseoglu, H. Kavas, B. Aktas, Phys. Status Solidi **203**, 1595–1601 (2006)
6. M.T. Farid, I. Ahmad, G. Murtaza, M. Kanwal, I. Ali, J. Ovonic Res. **12**(3), 137–146 (2016)
7. H.H. Joshi, R.G. Kulkarni, J. Mater. Sci. **21**, 2138–2142 (1986)
8. M.T. Farid, I. Ahmad, G. Murtaza, I. Ali, I. Ahmad, J. Chem. Soc. Pak. **38**(06), 1064–1072 (2016)
9. R.A. Brand, H. Georges-Gibert, J. Hubsch, J.A. Heller, J. Phys. F **15**, 1987–2007 (1985)
10. K.B. Modi, H.H. Joshi, R.G. Kulkarni, J. Mater. Sci. **31**, 1311–1317 (1996)
11. M.T. Farid, I. Ahmad, M. Kanwal, G. Murtaza, I. Ali, S.A. Khan, J. Magn. Magn. Mater. **428**, 136 (2017)
12. M.S. Shah, K. Ali, I. Ali, A. Mahmood, S.M. Ramay, M.T. Farid, Mater. Res. Bull. **98**, 77–82 (2018)
13. Y.-P. Fu, S.-H. Hu, Ceram. Int. **36**, 1311–1317 (2010)
14. I.H. Gul, E. Pervaiz, Mater. Res. Bull. **46**, 1353 (2012)
15. M. Hashim, K.S. Alimuddin, S.E. Shirsath, R.K. Kotnala, J. Shah, R. Kumar, Mater. Chem. Phys. **139**, 364 (2013)
16. H.M.T. Farid, I. Ahmad, K.A. Bhatti, I. Ali, S.M. Ramay, A. Mahmood, Ceram. Int. **43**, 7253–7260 (2017)
17. S.A. Saafan, S.T. Assar, B.M. Moharram, K. El Nimr, J. Magn. Magn. Mater. **322**, 628–632 (2010)
18. K.M. Batoo, Physics B **406**, 382–387 (2011)
19. M.T. Farid, I. Ahmad, M. Kanwal, G. Murtaza, I. Ali, M.N. Ashiq, S.A. Khan, J. Magn. Magn. Mater. **422**, 337–343 (2017)
20. K.K. Bamzai, G. Kour, B. Kaur, M. Arora, R.P. Pant, J. Magn. Magn. Mater. **345**, 255–260 (2014)
21. Z. Karimi, Y. Mohammad ifar, H. Shokrollahi, Sh. Khameneh Asl, Gh. Yousefi, L. Karimi, J. Magn. Magn. Mater. **361**, 150–156 (2014)
22. H.M.T. Farid, I. Ahmad, I. Ali, S.M. Ramay, A. Mahmood, G. Murtaza, J. Magn. Magn. Mater. **434**, 143–150 (2017)
23. M.T. Farid, I. Ahmad, M. Kanwal, Chin. J. Phys. **55**, 813–824 (2017)
24. M.A. Khan, M.U. Islam, M. Ishaque, I.Z. Rahman, Ceram. Int. **37**, 2519–2526 (2011)
25. A. Vasiliu, G. Maxim, M.L. Craus, E. Luca, Phys. Status Solidi A **13**, 371 (1972)
26. M.T. Farid, I. Ahmad, M. Kanwal, G. Murtaza, I. Ali, M.N. Ashiq, S.A. Khan, J. Electron. Mater. **46**, 1826–1835 (2017)
27. A. Iftikhar, M.U. Islam, M.S. Awan, M. Ahmad, S. Naseem, M.A. Iqbal, J. Alloys Compd. **601**, 116–119 (2014)
28. M.T. Farid, I. Ahmad, S. Aman, J. Chem. Soc. Pak. **35**(3), 793–799 (2013)